RESEARCH ARTICLE

Key Points:
- Upper tropospheric MOPITT CO agrees within ~10% with ACE-FTS and HIPPO-QCLS
- ACE-FTS apparent negative bias with respect to HIPPO-QCLS could be an artifact
- The MOPITT/ACE-FTS CO bias has remained mostly stable between 2004 and 2010

Supporting Information:
- Readme
- Text S1
- Table S1
- Table S2

Correspondence to:
S. Martínez-Alonso,
sma@ucar.edu

Comparison of upper tropospheric carbon monoxide from MOPITT, ACE-FTS, and HIPPO-QCLS

Sara Martínez-Alonso[1], Merritt N. Deeter[1], Helen M. Worden[1], John C. Gille[1], Louisa K. Emmons[1], Laura L. Pan[1], Mijeong Park[1], Gloria L. Manney[2], Peter F. Bernath[3], Chris D. Boone[4], Kaley A. Walker[5], Felicia Kolonjari[5], Steven C. Wofsy[6], Jasna Pittman[6], and Bruce C. Daube[6]

[1]Atmospheric Chemistry Division, National Center for Atmospheric Research, Boulder, Colorado, USA, [2]NorthWest Research Associates and Department of Physics, New Mexico Institute of Mining and Technology, Socorro, New Mexico, USA, [3]Department of Chemistry and Biochemistry, Old Dominion University, Norfolk, Virginia, USA, [4]Department of Chemistry, University of Waterloo, Waterloo, Ontario, Canada, [5]Department of Physics, University of Toronto, Toronto, Ontario, Canada, [6]Department of Earth and Planetary Science, Harvard University, Cambridge, Massachusetts, USA

Abstract Products from the Measurements Of Pollution In The Troposphere (MOPITT) instrument are regularly validated using in situ airborne measurements. However, few of these measurements reach into the upper troposphere, thus hindering MOPITT validation in that region. Here we evaluate upper tropospheric (~500 hPa to the tropopause) MOPITT CO profiles by comparing them to satellite Atmospheric Chemistry Experiment Fourier Transform Spectrometer (ACE-FTS) retrievals and to measurements from the High-performance Instrumented Airborne Platform for Environmental Research Pole to Pole Observations (HIPPO) Quantum Cascade Laser Spectrometer (QCLS). Direct comparison of colocated v5 MOPITT thermal infrared-only retrievals, v3.0 ACE-FTS retrievals, and HIPPO-QCLS measurements shows a slight positive MOPITT CO bias within its 10% accuracy requirement with respect to the other two data sets. Direct comparison of colocated ACE-FTS and HIPPO-QCLS measurements results in a small number of samples due to the large disparity in sampling pattern and density of these data sets. Thus, two additional indirect techniques for comparison of noncoincident data sets have been applied: tracer-tracer (CO-O_3) correlation analysis and analysis of profiles in tropopause coordinates. These techniques suggest a negative bias of ACE-FTS with respect to HIPPO-QCLS; this could be caused by differences in resolution (horizontal, vertical) or by deficiencies in the ACE-FTS CO retrievals below ~20 km of altitude, among others. We also investigate the temporal stability of MOPITT and ACE-FTS data, which provide unique global CO records and are thus important in climate analysis. Our results indicate that the relative bias between the two data sets has remained generally stable during the 2004–2010 period.

1. Introduction

The main sources of tropospheric carbon monoxide (CO) are incomplete fuel combustion, biomass burning, and oxidation of methane (CH_4) and other hydrocarbons; the main sink is oxidation by hydroxyl (OH). CO oxidation increases atmospheric carbon dioxide (CO_2) and tropospheric ozone (O_3); CO reduces OH levels, thus leading to enhanced concentrations of CH_4. As a result, CO emissions have a positive indirect radiative forcing of 0.23 W/m^2 (Intergovernmental Panel on Climate Change Fifth Assessment [*Myhre et al.*, 2013]). The mean lifetime of tropospheric CO is approximately 2 months. Because of its relatively short lifetime, CO is not well mixed, and thus it is often used to track polluted air masses in the troposphere [e.g., *Heald et al.*, 2003]. Tropospheric CO and CH_4 abundances control OH concentrations and, therefore, radical chemistry in the troposphere [*Jacob*, 1999].

CO and other species can be transported from the troposphere to the stratosphere via deep convection as well as by diabatic uplift in the tropical branch of the Brewer-Dobson circulation, as seen in the "tape recorder" phenomenon [*Schoeberl et al.*, 2006; *Randel et al.*, 2007]. The amount of CO transported into the stratosphere is estimated to be on the order of 100 Tg/yr [*Jacob*, 1999] or 5% of the global tropospheric production. CO loss in the stratosphere is mainly due to oxidation by OH and surpasses production, which is dominated by CH_4 oxidation.

The MOPITT (Measurements Of Pollution In The Troposphere) instrument on board NASA's Terra satellite has been measuring tropospheric CO since 2000, providing the longest global CO record to date. MOPITT

Table 1. Relevant Characteristics of the Data Sets Analyzed

Instrument	Data Availability	Horizontal Resolution (km)	Vertical Resolution (km)	Profiles Per Day
MOPITT	Mar 2000 to present	~22 (at nadir)	limited[b]	~200,000[c]
ACE-FTS	Feb 2004 to Aug 2010[a]	~300	~3–4	≤30
HIPPO-QCLS	1: Jan–Jun 2009	~0.16	~0.01	~6
	2: Oct–Nov 2009			
	3: Mar–Apr 2010			
	4: Jun–Jul 2011			
	5: Aug–Sep 2011			

[a]Geolocation information for each measurement in the occultations available.
[b]See section 2 for details.
[c]Clear-sky profiles.

retrievals have been validated against in situ measurements in the past [*Emmons et al.*, 2004, 2007, 2009; *Deeter et al.*, 2010, 2013, 2014]. Biases were generally found to be within the 10% required accuracy for both profiles and total column amounts [*Pan et al.*, 1995]. However, because few of the in situ profiles utilized reach into the upper troposphere (i.e., most NOAA flask sampling program flights only reach up to about 350–400 hPa), our understanding of MOPITT performance at low pressure levels is limited. Here we compare MOPITT retrievals to those of the ACE-FTS (Atmospheric Chemistry Experiment-Fourier Transform Spectrometer) instrument on board the SCISAT satellite, which has been measuring CO in the upper troposphere, stratosphere, and mesosphere since 2004 [*Bernath et al.*, 2005]. The ACE-FTS data set is unique for the purpose of this study given its high sensitivity to CO and satisfactory sampling density in the upper troposphere. A previous version of the ACE-FTS CO retrievals had been validated with respect to ground-based, airborne, and satellite measurements [*Clerbaux et al.*, 2008; *Hegglin et al.*, 2008]. These studies found that ACE-FTS uncertainties in the upper troposphere were less than 15% [*Clerbaux et al.*, 2008] and 9% [*Hegglin et al.*, 2008]. We also compare MOPITT and ACE-FTS retrievals to in situ measurements acquired by the QCLS (Quantum Cascade Laser Spectrometer) instrument [*Santoni et al.*, 2013; *McManus et al.*, 2010] during the HIPPO (High-performance Instrumented Airborne Platform for Environmental Research Pole to Pole Observations) experiment [*Wofsy et al.*, 2011]. HIPPO provides unparalleled high-resolution vertical profiles through the troposphere at all latitudinal and seasonal ranges, mostly over the Pacific region. Finally, we evaluate the temporal stability of MOPITT and ACE-FTS retrievals, important in climate analysis, during a 7 year (2004–2010) overlap period.

From the results of this analysis, our current understanding of CO abundances in the upper troposphere can be better assessed. Joint analyses of global, long-lived tropospheric and stratospheric CO data sets such as MOPITT and ACE-FTS can help clarify the mechanisms, magnitude, and variability of troposphere-stratosphere transport, which strongly influences the composition of the stratosphere.

Comparing the MOPITT, ACE-FTS, and HIPPO-QCLS data sets requires bridging large differences in their sampling resolution and observation types, as described in section 2. The methods used are introduced in section 3. The results from these comparisons are presented in section 4 and discussed in section 5. Section 6 summarizes our findings and conclusions.

2. Data Description

We compare CO measurements acquired by the MOPITT, ACE-FTS, and HIPPO-QCLS instruments (Table 1). MOPITT is a nadir-looking, cross-track scanning gas correlation radiometer on board NASA's EOS/Terra satellite that has been acquiring data since March 2000 [*Drummond and Mand*, 1996; *Drummond et al.*, 2010; *Worden et al.*, 2014]. Total CO column and vertical CO profiles are derived from its measurements in the near infrared (NIR) and thermal infrared (TIR). Vertical profiles with enhanced sensitivity to surface-level CO are produced from the simultaneous exploitation of both NIR and TIR bands [*Worden et al.*, 2010]. NIR measurements are only useful over land, while most HIPPO data were acquired over ocean; we thus analyze MOPITT CO data derived from the TIR channels only. Approximately 200,000 clear-sky MOPITT CO profiles, with horizontal resolution near 22 km at nadir, are retrieved daily; global coverage is achieved in ~3 days. Vertical profiles are provided on a 10-level pressure grid that extends from the surface to 100 hPa. The actual
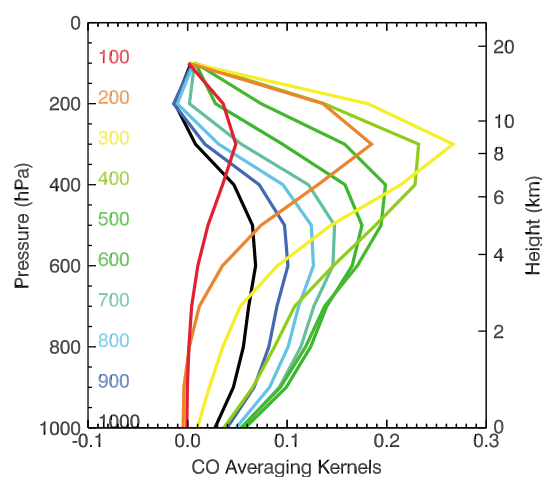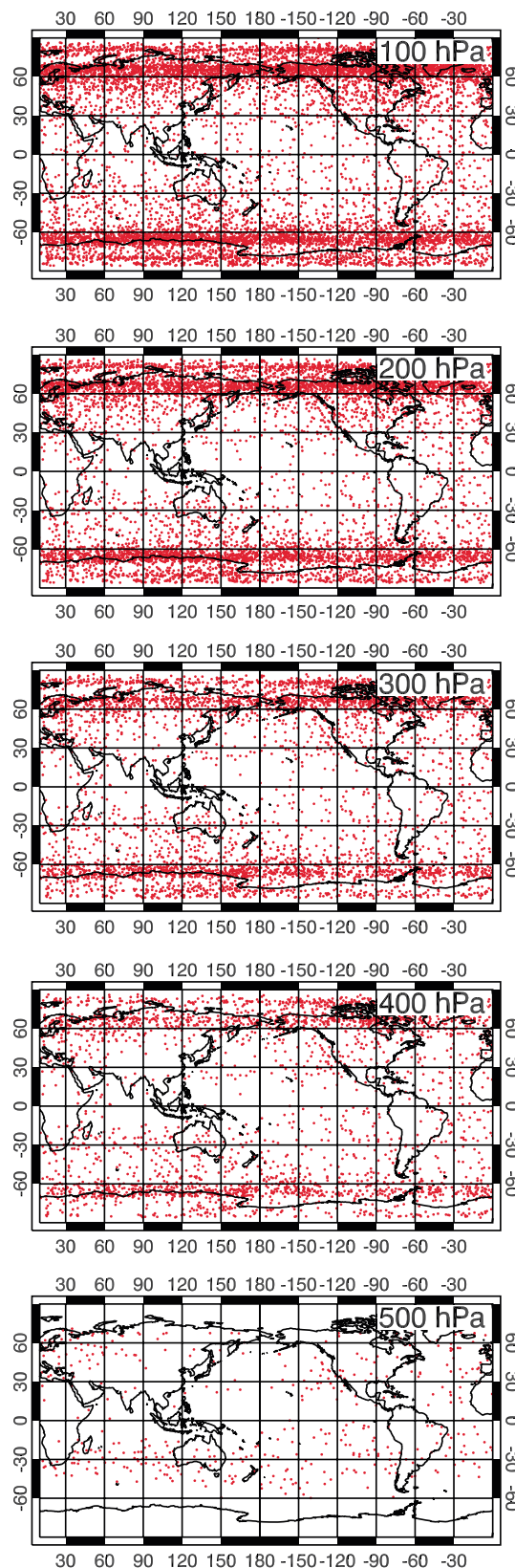
Figure 1. Example of mean averaging kernels for the MOPITT TIR-only product. They correspond to observations acquired on 10 April 2010 between 20°N and 24°N and −160°E and −156° E.

vertical resolution of the retrievals, given by their averaging kernels (Figure 1) [*Deeter et al.*, 2003; *Worden et al.*, 2010], is, however, more limited than that of the pressure grid. We use day-and-night, cloud-free, otherwise unfiltered MOPITT level 2 data from version 5 [*Deeter et al.*, 2013]. MOPITT data are corrected for a systematic geolocation error affecting versions 5 and earlier by shifting the reported longitude 0.35° to the east [*Deeter et al.*, 2014]. Our processing of the MOPITT data accounts for the fact that MOPITT retrievals from versions 4 and later are obtained using log normal a priori statistics [*Deeter et al.*, 2007], which represent the variability of tropospheric CO better than the VMR (volume mixing ratio) normal statistics.

ACE-FTS is a limb sounding, high-resolution (0.02 cm^{-1}) infrared spectrometer operating from 750 to 4400 cm^{-1}. It acquires up to 30 solar occultation measurements per day, providing highly accurate and precise self-calibrated transmittance spectra calculated using exoatmospheric solar spectra as the reference [*Boone et al.*, 2005]. Its horizontal resolution is typically on the order of 300 km, and its vertical resolution is approximately 3–4 km. Retrieved profiles are provided on both their original, occultation-dependent, irregular tangent grid and on an interpolated 1 km vertical grid with 150 fixed levels between 0.5 and 149.5 km. Actual sampling is performed down to the cloud tops or to ~5 km in the absence of clouds. We analyze all available level 2, 1 km vertical grid CO profiles derived from sunset and sunrise occultations from version 3.0 for which geolocation information as a function of altitude exists, encompassing the February 2004 to August 2010 period [*Boone et al.*, 2013]. Our analysis requires this information because ACE profiles show different degrees of slant depending on the occultation geometry, resulting in potentially large horizontal (latitudinal and longitudinal) offsets between individual measurements in a profile. We minimize the effect of the slant in ACE profiles when comparing them to those from MOPITT and HIPPO by using the geographical coordinates for each of the gridded levels in the ACE-FTS profiles. To avoid profiles with erroneous CO retrievals below 20.5 km (troposphere and lower stratosphere), we have filtered the data as described in the literature [*Tereszchuk et al.*, 2011; *Jones et al.*, 2012]. First, all profiles labeled "Do Not Use" in the ACE Data Issues List (https://databace.uwaterloo.ca/validation/data_issues_table.php) have been discarded. Profiles with anomalously low (below 0.1x median at each altitude) and high (>300 ppbv) CO concentrations have also been rejected (1.09 and 0.05% of profiles, respectively). Profiles with retrieval values smaller than their reported retrieval error and those with retrieval errors above 100x the Median Absolute Deviation of the retrieval errors at any given altitude below 20.5 km have also been discarded (0.21 and 1.56% of profiles).

The HIPPO experiment [*Wofsy et al.*, 2011] consisted of airborne measurements of cross sections of atmospheric concentrations pole-to-pole, mostly over the Pacific Ocean and North America, from the surface to the tropopause and into the lower stratosphere over high latitudes. It comprised five separate field campaigns during the 2009 to 2011 period, totaling more than 750 profiles (people.seas.harvard.edu/~swofsy/HIPPO_merge_1s.20120827.1558.tar.gz, retrieved 4 September 2012). Here we analyze CO measurements acquired by the QCLS instrument [*McManus et al.*, 2010; *Santoni et al.*, 2013], performed at 1 Hz sampling rate with precision and accuracy of 0.15 and 3.5 ppb, respectively. O_3 measurements from the NOAA-Chemical Sciences Division Dual-Beam Ultraviolet Absorption Ozone Photometer [*Proffitt and McLaughlin*, 1983] are also utilized (1 Hz sampling rate; 1–2 ppbv precision at 5–10 km, respectively; 5% accuracy). The vertical resolution of HIPPO measurements is ~10 m, and each data point represents a linear distance of ~160 m. Due to its resolution, precision, and accuracy, we consider the HIPPO measurements our "truth." HIPPO sampled the vertical extent of the troposphere via steep, linear flights rather than spirals, with an average horizontal extent ranging from 25 to 940 km. We minimize the

effect of the slant in HIPPO profiles when comparing them to profiles from the other instruments by taking into consideration the geographic location and altitude of each individual measurement.

3. Methods

3.1. MOPITT-ACE Comparison

MOPITT and ACE-FTS data were paired for direct profile comparison according to date and location (≤12 h apart, ≤200 km radial distance [*Deeter et al.*, 2013]). For pairing purposes, each ACE -FTS profile was assigned the averaged latitude and longitude of its relevant individual measurements (i.e., measurements with valid CO retrievals and within the MOPITT vertical range). Figure 2 shows the geographical distribution of valid MOPITT/ACE-FTS pairs at different MOPITT pressure levels. The marked latitudinal difference in pair density results from ACE's high-inclination orbit, which favors coverage at high latitudes. The decreasing number of pairs with increasing pressure is due to the fact that ACE-FTS performs no measurements below the top of the clouds. Compared to profiles from both in situ and limb-sounding instruments, MOPITT-retrieved profiles exhibit coarse vertical resolution [*Deeter et al.*, 2013, and references therein]. For optimal estimation-based retrieval algorithms, such as MOPITT's, retrieved products may also incorporate a significant amount of a priori information. Therefore, to validate MOPITT data using a data set with much higher vertical resolution, it is important to distinguish differences associated with (1) the expected effects of differing vertical resolution and a priori inclusion from (2) all other potential sources of retrieval bias. This is achieved by explicitly accounting for the smoothing effect, as quantified by the MOPITT averaging kernel matrix, and the dependence of MOPITT retrieved profiles on the a priori profile [*Rodgers and Connor*, 2003].

Figure 3 shows an example of colocated MOPITT and ACE-FTS CO profiles and illustrates the process followed to match their vertical sampling (smoothing). First, all the MOPITT profiles coinciding in space and time with a

Figure 2. Geographic distribution of colocated (≤12 h apart, ≤200 km radial distance) MOPITT and ACE-FTS CO retrievals as a function of MOPITT pressure level.

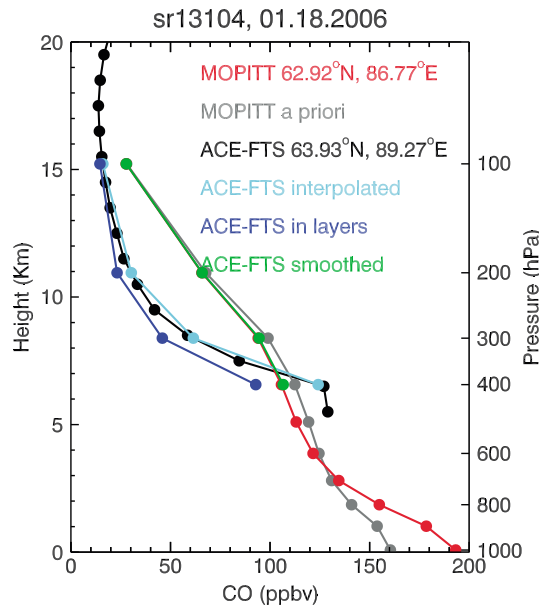**Figure 3.** Example of colocated MOPITT (red) and ACE-FTS (black) CO profiles to illustrate the smoothing process. The original ACE-FTS profile is interpolated (cyan) to match the MOPITT vertical resolution, averaged (dark blue) to fit the MOPITT layering scheme and convolved (green) with the a priori (gray) and averaging kernels from MOPITT.

single ACE-FTS profile were identified. The ACE-FTS profile was then interpolated to match the pressure levels in the MOPITT data set and averaged according to the MOPITT layering scheme, by which each retrieval level corresponds to a uniformly weighted layer immediately above that level [*Deeter et al.*, 2013]. To avoid artifacts, missing individual measurements in the ACE-FTS profile were substituted by the corresponding MOPITT a priori; the smoothed values resulting from such substitutions were excluded from subsequent analyses. Next, for each colocated MOPITT profile, the observation operator **H** (its averaging kernel and a priori constraint) was applied to the ACE-FTS profile as described in *Rodgers and Connor* [2003]:

$$\boldsymbol{H}X_{\mathrm{HVR}} = X_{\mathrm{LVR\ apriori}} + \mathrm{AK}_{\mathrm{LVR}}\left(X_{\mathrm{HVR}} - X_{\mathrm{LVR\,apriori}}\right) \quad (1)$$

where LVR and HVR indicate low- and high-vertical resolution instruments, respectively (MOPITT and ACE-FTS, in this case), AK is the averaging kernel (Figure 1), X the CO retrieved profile, and $\boldsymbol{H}X_{\mathrm{HVR}}$ indicates the result of applying the observation operator (This expression is commonly used to compare satellite data to in situ [e.g., *Emmons et al.*, 2009] and model [e.g., *Jiang et al.*, 2013] profiles.).

The MOPITT/ACE-FTS pairing was then further refined by rejecting individual ACE measurements whose horizontal distance from the averaged MOPITT profile was above the 200 km threshold.

Finally, the percentage bias between LVR and HVR retrievals was quantified as follows:

$$\mathrm{Bias} = \sum_{i=1}^{m} \frac{\sum_{j=1}^{n} \dfrac{X_{\mathrm{LVR}\,j} - \boldsymbol{H}_j X_{\mathrm{HVR}\,i}}{\left(X_{\mathrm{LVR}\,j} + \boldsymbol{H}_j X_{\mathrm{HVR}\,i}\right)/2} \times 100/n}{m} \quad (2)$$

where m is the number of HVR profiles, n is the number of LVR profiles colocated to each HVR profile, and $\boldsymbol{H}_j X_{\mathrm{HVR}\,i}$ indicates HVR profile i smoothed with respect to LVR profile j. (A computationally less costly approximation method for bias calculation, relevant for MOPITT Level 3 data analysis, is discussed in the supporting information.).

3.2. MOPITT-HIPPO Comparison

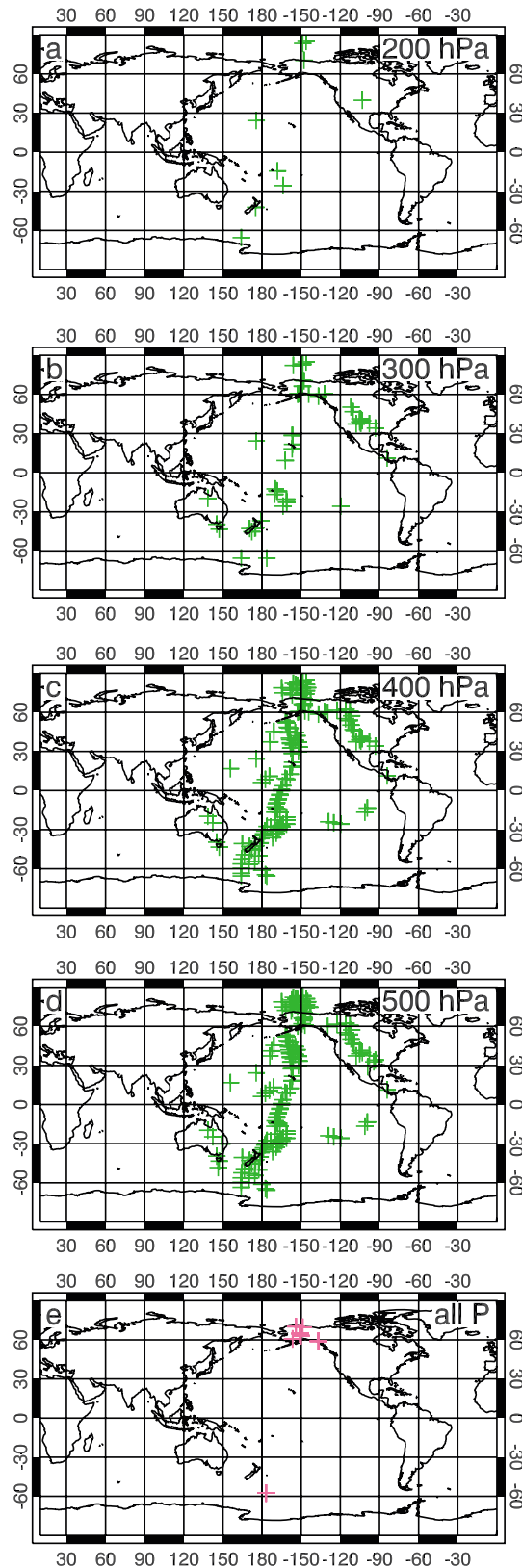We compared MOPITT and HIPPO profiles that were acquired ≤12 h and ≤200 km apart for self-consistency and for consistency with previous work [*Deeter et al.*, 2013]. For pairing purposes and to minimize the effect of the slant (divergence from the vertical) in HIPPO profiles, the latitude and longitude of relevant individual measurements in each HIPPO profile (i.e., those with valid CO data) were averaged and the result was assigned to the profile. The spatial distribution of paired MOPITT and HIPPO-QCLS profiles at MOPITT equivalent pressures between 200 and 500 hPa is shown in Figures 4a–4d. No pairs were found at the 100 hPa level. The paired samples distribution mimics the pattern of the HIPPO flight paths. The decreasing number of pairs with decreasing pressure is due to fewer HIPPO-QCLS measurements at higher altitudes.

Each HIPPO profile was interpolated to the MOPITT pressure levels, and the MOPITT layering scheme was replicated as described earlier. To avoid the systematic loss of the last (first) layer in each HIPPO profile,

we determined whether the actual HIPPO measurements reached the *P* level at the base (top) of the layer minus (plus) 50 hPa, in which case we assigned to that last (first) layer the average of the measurements between the base (top) of the layer and the top (bottom) of the profile. To avoid spurious results from the smoothing process, we substituted the corresponding MOPITT a priori value for missing HIPPO values; the smoothed values directly resulting from such substitutions were excluded from subsequent analyses. The HIPPO profiles were then convolved using equation (1). The results of this process are shown in Figure 5. To minimize the effect of the slant in HIPPO profiles, MOPITT-HIPPO distances at the center of each pressure layer were calculated and individual measurements more than 200 km apart were discarded. Lastly, the percentage bias between paired MOPITT and HIPPO-QCLS retrievals was calculated using equation (2).

3.3. ACE-HIPPO Comparison

Direct profile comparison between the ACE-FTS and HIPPO-QCLS data sets is challenging because of the nonhomogeneous sampling pattern of the former and the sparsity in space and time of the latter. To complement the direct comparison of profiles from these instruments, we have applied two additional indirect techniques which suppress the effects of geophysical variability and, thus, provide "instantaneous climatologies" [*Hegglin et al.*, 2008, 2009]: tracer-tracer (CO-O_3) correlation analysis and analysis of profiles relative to the thermal tropopause.

3.3.1. Direct Profile Comparison

To minimize the effect of the large slant in profiles from both instruments, we identified profiles with matching individual measurements as follows. First, we filtered all possible pairs of measurements according to date (± 3 days apart) and spatial proximity (≤200 km horizontally and ≤1 km vertically); valid pairs were flagged for further processing. (Given the fact that in the upper troposphere (1) horizontal air velocities outside of the jets are moderate (0–20 m/s), and (2) outside of the polar vortex, air masses with

Figure 4. (a–d) Geographic distribution of colocated (≤12 h apart, ≤200 km radial distance) MOPITT and HIPPO-QCLS CO retrievals as a function of MOPITT pressure level. (e) Map showing the location of colocated (±3 days apart, ≤200 km radial distance) ACE-FTS and HIPPO-QCLS CO profiles.
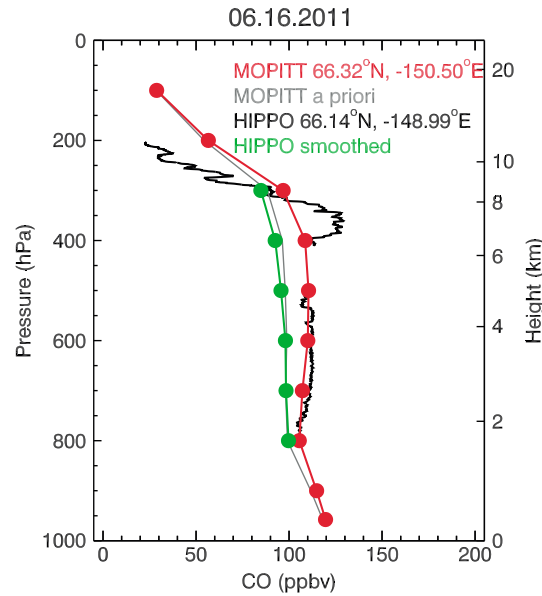
Figure 5. Example of colocated MOPITT (red) and HIPPO-QCLS (black) CO profiles. The smoothed HIPPO-QCLS profile (green) was obtained applying a priori (gray) and averaging kernels from MOPITT. Intermediate results of the smoothing process similar to those shown in Figure 3 are not included for clarity.
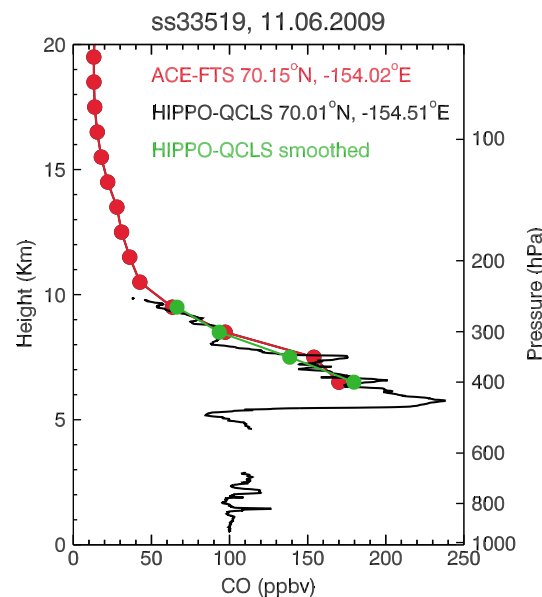

Figure 6. Example of colocated ACE-FTS (red) and HIPPO-QCLS (black) CO profiles. The smoothed HIPPO-QCLS profile (green) was obtained applying a triangular function. Intermediate results of the smoothing process similar to those shown in Figure 3 are not included for clarity.

contrasting CO are generally extensive (thousands of kilometers across, as shown by MOPITT maps), then 3 days is a reasonable colocation time threshold.) A modest number of paired ACE-HIPPO profiles with matching individual measurements were identified: one corresponds to HIPPO campaign 1, seven to HIPPO 2, and one to HIPPO 3. Due to unavailability at the time of writing of geolocation information as a function of altitude for ACE occultations acquired after August 2010, direct profile comparison for HIPPO 4 and 5 was not possible. The geographic location of successfully paired ACE-HIPPO profiles is shown in Figure 4e; they are mostly restricted to high latitudes, where ACE sampling is more frequent.

Since averaging kernels are not available for the ACE retrievals [*Dupuy et al.*, 2009], HIPPO profiles with flagged measurements were smoothed to approach ACE-FTS's lower vertical resolution by using a triangular function as described in *Dupuy et al.* [2009]:

$$X_{\text{smoothed}}(z_i) = \frac{\sum_{j=1}^{n} w_j(z_j - z_i) \cdot X(z_j)}{\sum_{j=1}^{n} w_j(z_j \text{-} z_i)} \qquad (3)$$

where w is a triangular weight function of full width at the base equal to 3 km (to account for the limited vertical resolution of the instrument [*Dupuy et al.*, 2009]) centered at height z_i, n is the number of measurements in the profile inside the full width of the function, and $X(z_j)$ is the retrieved VMR at height z_j. Figure 6 illustrates the smoothing process. Individual measurements in the smoothed profiles exceeding the distance thresholds were removed. Finally, percentage bias was calculated as follows:

$$\text{Bias} = \sum_{i=1}^{m} \frac{X_{\text{LVR } i} - X_{\text{HVR smoothed } i}}{(X_{\text{LVR } i} + X_{\text{HVR smoothed } i})/2} \times 100/m$$

$$(4)$$

where m is the number of paired ACE-HIPPO measurements.

3.3.2. Tracer-Tracer Correlation Analysis

This indirect technique, which allows comparison of noncoincident data sets [*Fischer et al.*, 2000; *Tilmes et al.*, 2010], has been previously used for model and instrument validation [*Pan et al.*, 2007; *Hegglin et al.*, 2008, 2009]. The mixing ratios of
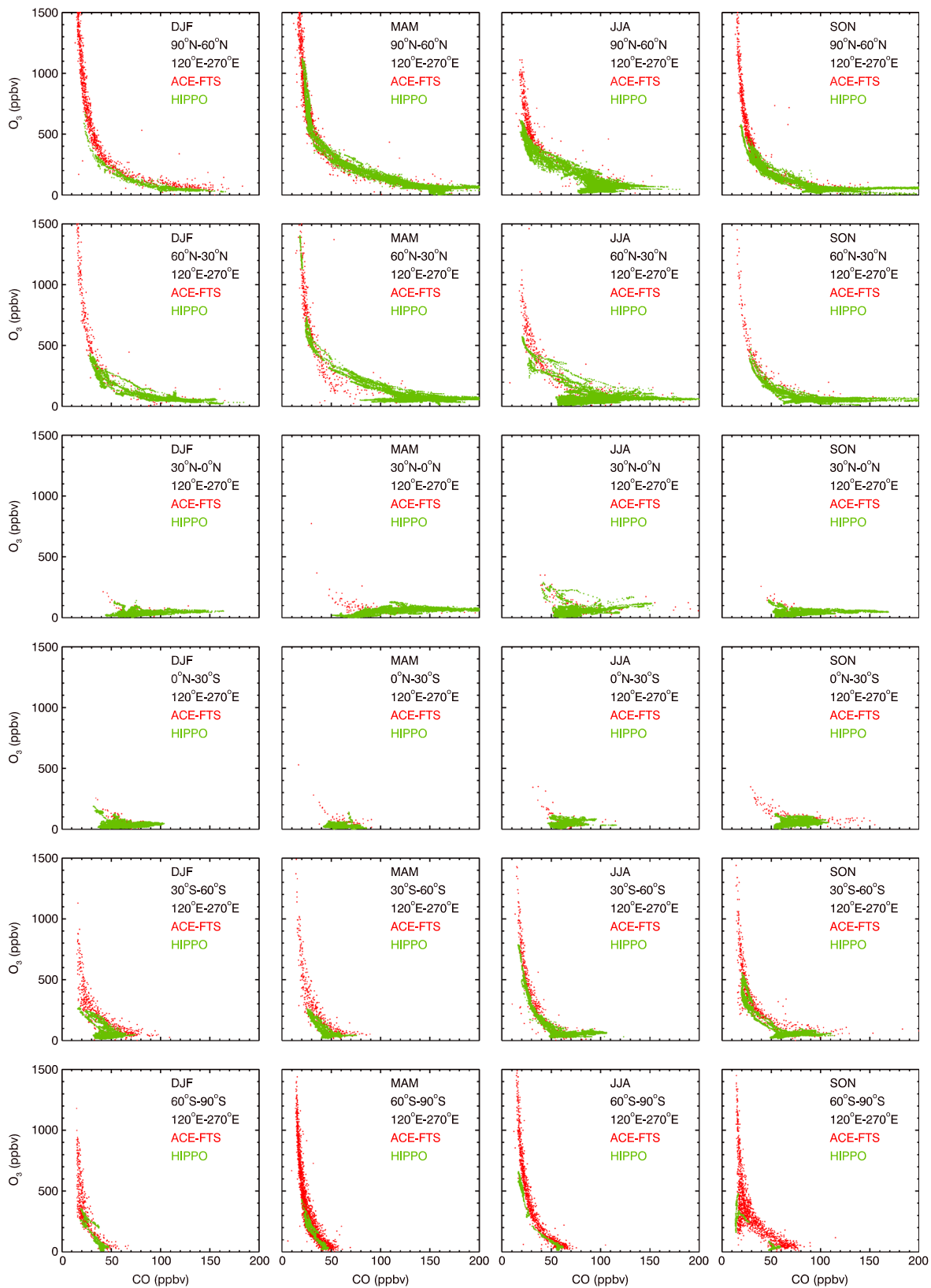
Figure 7. Tracer-tracer (CO-O$_3$) correlation scatterplots for ACE-FTS (red) and HIPPO (green), segregated by season and latitude. Only ACE-FTS data between 120°E and 270°E were included to match the longitudinal extent of the HIPPO mission. DJF = December−January−February, MAM = March−April−May, JJA = June−July−August, and SON = September−October−November.
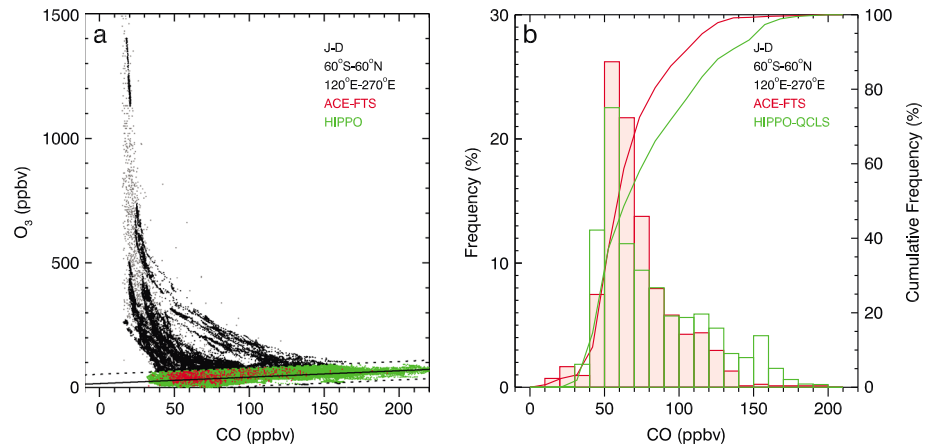
Figure 8. (a) CO-O_3 tracer-tracer correlation scatterplot for ACE-FTS (gray and red) and HIPPO (black and green). Only ACE-FTS data between 120°E and 270°E were included to match the longitudinal extent of the HIPPO campaigns. Data poleward of ±60° latitude were rejected to minimize differences in latitudinal sampling between the two instruments. The solid line indicates a first-degree polynomial fitted to the background tropospheric air measurements, corresponding to $O_3 \leq 100$ ppbv (see text for details). Dotted lines indicate 3 sigma standard deviations; data points within them are considered tropospheric measurements. JD = January to December. (b) Frequency distribution and cumulative histogram of tropospheric CO measurements according to ACE-FTS (red) and HIPPO-QCLS (green).

species such as CO and O_3 have strong, contrasting gradients at the tropopause. Thus, scatterplot representations of their abundances can be used to identify and separate tropospheric and stratospheric samples for further analysis of these populations. Here we present, first, results based on CO and O_3 measurements from the ACE-FTS and HIPPO data sets acquired between February 2004 and August 2010 (for ACE) and between January 2009 and September 2011 (for HIPPO). Only ACE-FTS retrievals between 120°E and 270°E were utilized to sample the same longitudinal range as HIPPO. The full vertical resolution of the HIPPO profiles was preserved (i.e., no smoothing was applied). Retrievals were segregated according to location and season to minimize latitude- and time-dependent changes in the tracer profiles. The resulting CO versus O_3 scatterplots are shown in Figure 7. Then, to better qualify the level of agreement between the two data sets as well as to focus on tropospheric values, their frequency distributions were characterized as follows. To retain enough measurements, samples from all seasons and latitudes were grouped together. Only data between 8 January 2009 and 16 April 2010 and between −60° and 60° latitude were utilized for optimal temporal and spatial overlap and to avoid differences in sampling density between the two data sets caused by ACE's preferential sampling of high latitudes. Then, to extract the tropospheric measurements, the method described in *Pan et al.* [2004] was applied. First, all measurements associated with O_3 greater than 100 ppbv [*Hegglin et al.*, 2009], indicative of background stratospheric air, were discarded. A higher O_3 threshold than that proposed by *Pan et al.* [2004] (70 ppbv) was used to account for the ~18% ACE-FTS O_3 high bias in the troposphere [*Hegglin et al.*, 2008]. Next a first-degree polynomial line was fitted to the remaining measurements, representative of
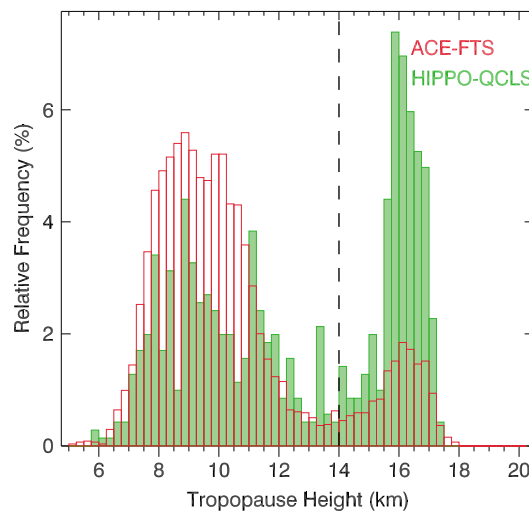

Figure 9. Frequency distribution of thermal tropopause heights derived from GEOS-5 data for ACE-FTS (red) and HIPPO-QCLS (green) CO profiles. The frequency distributions for both instruments are very similar and clearly bimodal, with a threshold near 14 km separating the extratropical tropopause population (lower heights) from the tropical tropopause population (higher heights). ACE-FTS does not sample the tropics as frequently as HIPPO, hence the difference in magnitude between the peaks near 16 km.
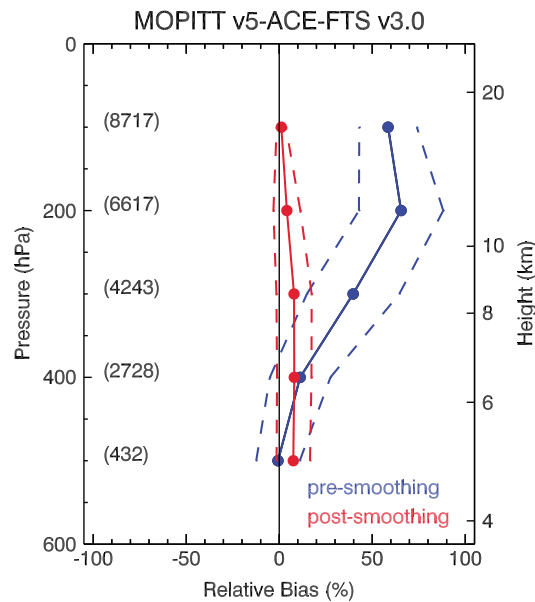
Figure 10. Average percent bias between all colocated MOPITT and ACE-FTS retrievals as a function of MOPITT pressure level. Blue and red indicate bias before and after ACE-FTS smoothing, respectively. Numbers in parenthesis are the number of valid MOPITT-ACE measurements pairs at each pressure level. Dashed lines show ±1 standard deviation from the average.

background tropospheric air (Figure 8a). Frequency and cumulative histograms were calculated for the data points within 3 sigma of the fitted line (Figure 8b). These data points are considered to be tropospheric measurements.

3.3.3. Profiles in Tropopause Coordinates

Comparison of profiles relative to the thermal tropopause is another indirect technique that is useful for the analysis of noncoincident data sets in the upper troposphere–lower stratosphere [*Hegglin et al.*, 2008, 2009, and references therein; *Tilmes et al.*, 2010]. The thermal tropopause is defined as the lowest level at which the lapse rate decreases to 2°C/km or less; additionally, the average lapse rate between this level and all higher levels within 2 km should not exceed 2°C/km [*World Meteorological Organization*, 1957]. Segregating profiles according to their thermal tropopause height insures that similar samples are compared together, since it separates stratospheric from tropospheric air masses as well as tropical from extratropical air masses. Trace gas profiles expressed in tropopause coordinate space show a more compact distribution than their equivalents in actual altitude space, thus allowing for more meaningful averaging in geographical space and/or time.
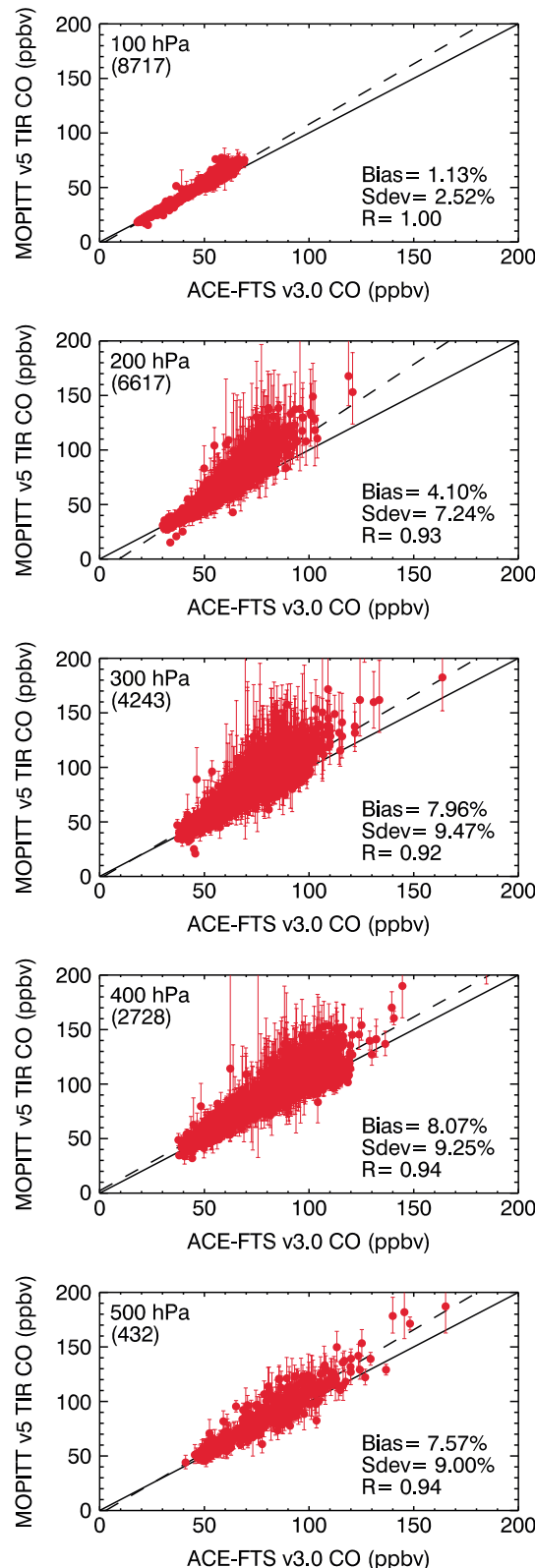
In this analysis, the height of the thermal tropopause for each ACE-FTS and HIPPO profile was derived from temperatures interpolated to the measurement locations from the Goddard Earth Observing System version 5 (GEOS-5) data assimilation system [*Manney et al.*, 2007, 2011]. (Both the HIPPO and ACE-FTS data sets include temperature profiles. However, ACE-FTS temperature values for altitudes ≤15 km are derived from meteorological data rather than retrieved. Thus, to preserve intraprofile and interprofile consistency, GEOS-5 temperature data are used for both instruments.) ACE-FTS profiles outside the 120°E to 270°E longitude range were excluded for consistency with the longitudinal extent of the HIPPO campaigns; we utilized all available data regardless of their date. Figure 9 shows the frequency distribution of thermal tropopause heights for CO profiles from the two instruments. Both distributions are clearly bimodal, with a threshold near 14 km that separates profiles from tropical latitudes (high tropopause) from those from extratropical latitudes

Table 2. Statistics of CO Percent Bias Between MOPITT and ACE-FTS and Between MOPITT and HIPPO-QCLS

MOPITT *P* Level (hPa)	MOPITT Versus ACE-FTS		MOPITT Versus HIPPO-QCLS	
	Percent Difference	Percent Standard Deviation	Percent Difference	Percent Standard Deviation
100	58.5[a] (1.1)[b]	15.5[a] (2.5)[b]	-[a] (-)[b]	-[a] (-)[b]
200	65.5 (4.1)	22.7 (7.2)	56.5 (11.0)	31.7 (8.8)
300	39.7 (8.0)	24.8 (9.5)	30.1 (13.6)	24.1 (10.2)
400	11.2 (8.1)	16.3 (9.2)	4.6 (3.8)	18.4 (10.7)
500	−0.7 (7.6)	11.7 (9.0)	−4.5 (−1.2)	14.4 (10.3)
600	- (-)	- (-)	−5.0 (−3.2)	14.8 (10.3)
700	- (-)	- (-)	−2.5 (−3.9)	14.9 (10.5)
800	- (-)	- (-)	0.8 (−3.1)	14.4 (10.6)
900	- (-)	- (-)	6.3 (−1.3)	15.5 (10.2)
1000	- (-)	- (-)	8.7 (0.9)	20.8 (9.2)

[a]Values obtained before smoothing.
[b]Values in parentheses were obtained after smoothing the higher vertical resolution profiles with the MOPITT averaging kernels and a priori.

(low tropopause). ACE-FTS and HIPPO-QCLS CO profiles from each of the two populations were transformed, so their height was expressed in tropopause coordinates and averaged. The relative bias between the average profiles of the two instruments for each population was then calculated.

4. Results

Next we present results obtained from direct profile comparison of all three data sets as well as (for ACE-FTS versus HIPPO-QCLS) from tracer-tracer (CO-O_3) correlation analysis and from analysis of profiles in tropopause coordinates. Unless noted otherwise, the comparisons reported were performed after smoothing of the higher vertical resolution data set.

4.1. MOPITT-ACE Results

Results from the MOPITT to ACE-FTS direct profile comparison, expressed as relative bias, are summarized in Figure 10 and Table 2. The number of paired samples at MOPITT pressure levels between 100 and 500 hPa ranges from 8717 to 432. After-smoothing bias values range between 1 and 8%, with 1 sigma standard deviation below 10%. Overall, biases both before and after smoothing are positive, with the MOPITT retrievals being higher.

We can extend the comparison between these two data sets by examining MOPITT and smoothed ACE-FTS retrieval pairs at each relevant MOPITT-equivalent pressure level as shown in Figure 11. Both sets of retrievals are strongly correlated between 100 and 500 hPa (R values in the 0.92 to 1 range). The best match between the two data sets occurs at 100 hPa, where the bias is slightly above 1% and the 1 sigma standard deviation is 2.5%. The paired samples cover substantial ranges of CO (from ~55 ppbv wide at 100 hPa to ~150 ppbv wide at 400 hPa), thus representing diverse atmospheric compositions.

4.2. MOPITT-HIPPO Results

Results from the comparison between the two data sets, expressed as relative bias, are shown in

Figure 11. Scatterplots showing colocated MOPITT and smoothed ACE-FTS CO retrievals as a function of MOPITT pressure level. Vertical bars indicate ±1 standard deviation from the mean. Solid lines show the ideal one-to-one relationship, and dashed lines the least squares best fit.
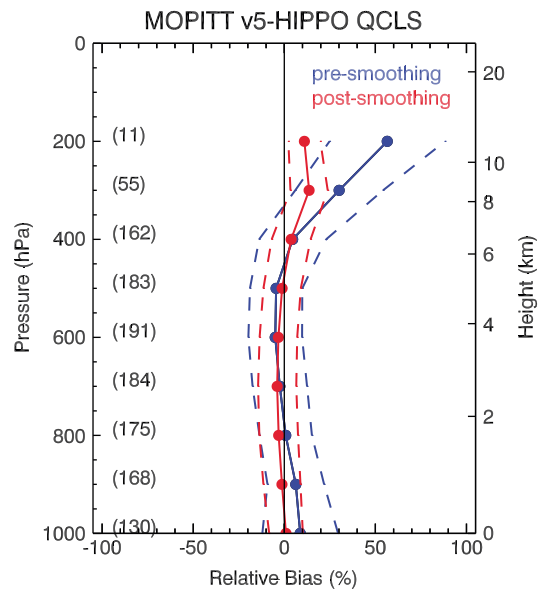
Figure 12. Average percent bias between all colocated MOPITT and HIPPO-QCLS measurements as a function of MOPITT pressure level. Blue and red indicate bias before and after HIPPO-QCLS smoothing, respectively. Numbers in parenthesis are the number of valid MOPITT-HIPPO measurements pairs at each pressure level. Dashed lines show ±1 standard deviation from the average.

Figure 12 and Table 2. Even though the number of paired samples in the upper troposphere (between 183 and 11 at 500 and 200 hPa, respectively) is much more modest than in the MOPITT versus ACE-FTS comparison, paired samples are still representative of diverse atmospheric compositions, as suggested by their geographic distribution (Figure 4) and seen in the large range of CO abundances (Figure 13). The width of the CO ranges represented by the paired samples is between ~50 and ~110 ppbv at 200 and 500 hPa, respectively (Figure 13). Smoothed HIPPO-QCLS and MOPITT retrievals are particularly similar between 500 and 1000 hPa, with bias between −4 and +1% and 1 sigma standard deviation near 10%. At lower pressure levels (400 to 200 hPa), the bias increases slightly, reaching positive values (i.e., MOPITT retrievals are higher) between 4 and 14%, with 1 sigma standard deviation also near 10%.

CO retrieval scatterplots (Figure 13) at relevant MOPITT-equivalent pressure levels show a strong correlation between the two data sets (R values between 0.87 and 0.97).

4.3. ACE-HIPPO Results

Bias values obtained from direct profile comparison are summarized in Figure 14 and Table 3. Postsmoothing bias increases with decreasing pressure, ranging between −1% (at ~490 hPa) and −37% (at ~170 hPa) (i.e., ACE-FTS retrievals appear to be lower); 1 sigma standard deviation values average ~23%. The number of paired measurements at each pressure level is notably low (from 3 to 6). As shown in Figure 4e, paired profiles are concentrated at high latitudes over North America and the South Pacific due to denser ACE sampling poleward and to the limited HIPPO longitudinal range. Figure 15 shows the strong correlation ($R = 0.94$) found in the direct comparison of ACE-FTS and smoothed HIPPO-QCLS CO retrievals. In general, ACE-FTS values are lower than their HIPPO-QCLS counterparts. Although the number of samples is very modest (36 pairs of individual measurements in total), they represent a substantial range of atmospheric compositions, with CO abundances ranging from ~20 to ~200 ppbv.

The results from the tracer-tracer (CO-O_3) correlation analysis provide complementary evidence as to the level of agreement between ACE-FTS and nonsmoothed HIPPO-QCLS CO retrievals. Figures 7 and 8a show the typical L shape of CO versus O_3 distributions given by the tropospheric and stratospheric branches, characterized by mostly constant O_3 and CO values, respectively. A wide transition zone between them corresponds to mixing of tropospheric and stratospheric air [*Fischer et al.*, 2000]. Figure 7 shows that overall, the overlap between the two data sets in tracer-tracer space is satisfactory. The HIPPO-QCLS data lie, in general, within the range of the ACE-FTS data. Both data sets show fine-detailed features such as the "spur" in the September–October–November data poleward of 60°S. The highest O_3 values, indicative of stratospheric air, are rarely present in the aircraft data due to flight height limitations. However, when they are (e.g., March–April–May data poleward of 30°N), they match the satellite O_3 values particularly well. The lower number of ACE measurements between 30°N and 30°S, though, hinders the comparison at low latitudes. Figure 8b shows the frequency and cumulative frequency distributions of tropospheric CO (i.e., CO retrievals associated with low O_3 values) according to ACE-FTS and HIPPO-QCLS. The distributions of the two instruments appear similar, in general, having the same shape and mode. However, high (>100 ppbv) CO
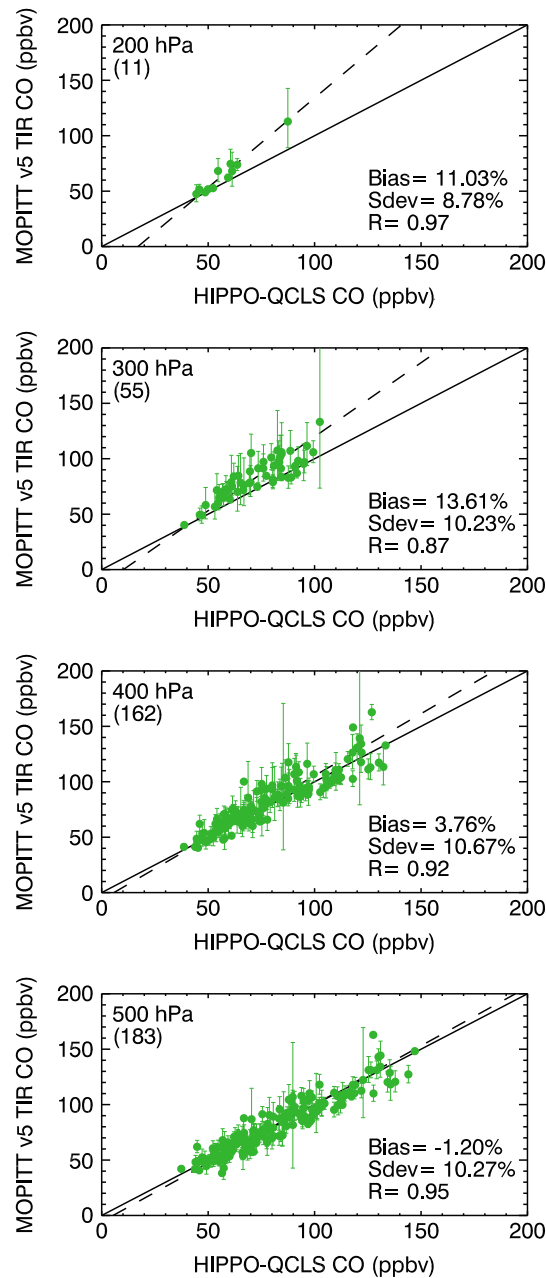
Figure 13. Scatterplots showing colocated MOPITT and smoothed HIPPO-QCLS retrievals as a function of MOPITT pressure level. Vertical bars indicate ±1 standard deviation from the mean. Solid lines show the ideal one-to-one relationship, and dashed lines the least squares best fit.

values are more frequent in the HIPPO-QCLS data set (~25% of the measurements) than in the ACE-FTS data set (~12%).

Lastly, results obtained from the comparison of ACE-FTS and HIPPO-QCLS CO profiles in tropopause coordinates are summarized in Figure 16; data were segregated according to thermal tropopause height as explained in section 3.3.3. The number of samples from each data set varies widely, ranging from less than 10 to a few thousands, depending on altitude. For extratropical profiles (i.e., profiles with thermal tropopause below or at 14 km, Figure 16a) all biases from the tropopause downward are negative; that is, ACE-FTS CO retrievals are lower than their HIPPO-QCLS counterparts. The average bias value between the tropopause and 8 km below it is −21%. For tropical profiles (i.e., profiles with thermal tropopause above 14 km, Figure 16b), biases range
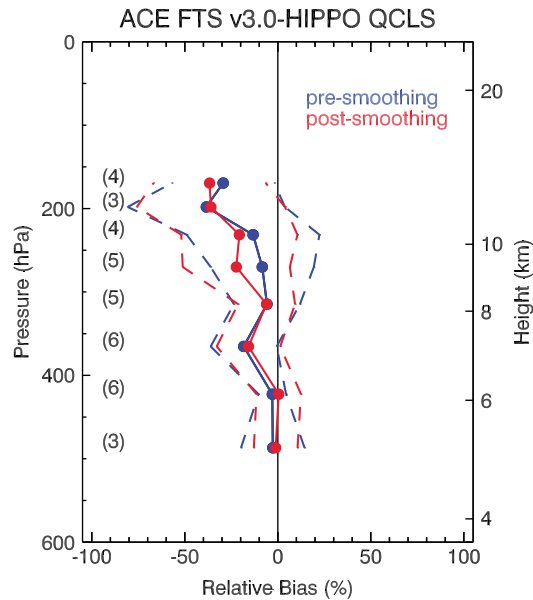
Figure 14. Average percent bias between all colocated ACE-FTS and HIPPO-QCLS measurements as a function of ACE height. Blue and red indicate bias before and after HIPPO-QCLS smoothing, respectively. Numbers in parenthesis are the number of valid ACE-HIPPO measurements pairs at each height level. Dashed lines show ±1 standard deviation from the average.

between −21% (at the tropopause) and +20% (12 km below the tropopause). Figure 17 shows results obtained by subsetting the profiles according to both thermal tropopause height and season. Similar trends to those just discussed are seen in most individual seasons: Negative biases are predominant for profiles with tropopauses at or below 14 km. Profiles with tropopauses above 14 km show negative biases near the tropopause, approach 0 bias near ~5 km below the tropopause, and, in some cases, have positive biases further below. Profiles from the December–January–February season depart from this general behavior.

4.4. Trend in MOPITT-ACE Bias

The long life spans and substantial overlap in time between the MOPITT and ACE-FTS data sets offer a good opportunity to investigate their long-term relative behavior. Figure 18 summarizes the results of our bias trend analysis at different pressure levels for the 2004–2010 period; positive values indicate that MOPITT retrievals are higher than those from ACE-FTS. No seasonal trends are apparent, and fit lines calculated for pressure levels between 100 to 400 hPa are very close to flat (i.e., no strong time bias trends are apparent). Slope values are very low, ranging from −0.05% bias/yr to 0.23% bias/yr. The fit line derived for the 500 hPa level does show a slightly stronger slope of −0.85% bias/yr.

Table 3. Statistics of CO Percent Bias Between ACE-FTS and HIPPO-QCLS

ACE Height, P Level (km, hPa)	Difference (%)	Standard Deviation (%)
12.5, 169	−29.4[a] (−36.7)[b]	27.5 (30.2)
11.5, 198	−38.4 (−36.0)	42.3 (39.8)
10.5, 231	−13.3 (−20.7)	35.6 (31.2)
9.5, 270	−8.4 (−22.3)	27.7 (28.8)
8.5, 315	−5.8 (−6.0)	17.8 (15.3)
7.5, 365	−18.4 (−15.8)	17.7 (17.1)
6.5, 423	−3.0 (0.5)	7.4 (11.9)
5.5, 487	−2.7 (−1.2)	17.1 (11.7)

[a]Values obtained before smoothing.
[b]Values in parentheses were obtained after smoothing the HIPPO-QCLS profiles with a triangular function.
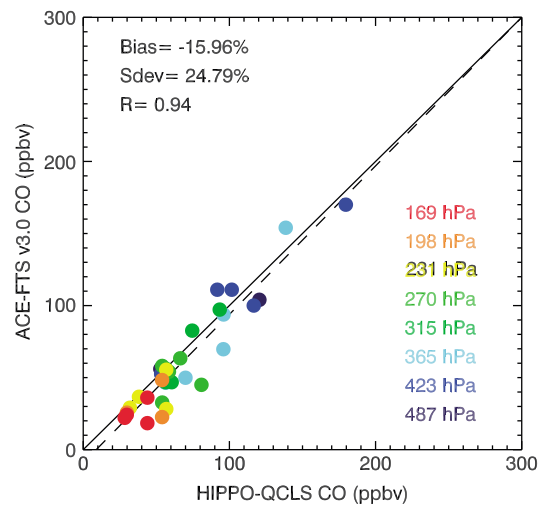
Figure 15. Scatterplot showing colocated ACE-FTS CO and smoothed HIPPO-QCLS measurements as a function of ACE pressure level. Solid lines show the ideal one-to-one relationship, and dashed lines the least squares best fit.

5. Discussion

According to our results, upper tropospheric MOPITT CO retrievals show a slight (in the <1 to 8% range) positive bias with respect to ACE-FTS (Figure 10). Both the number of paired measurements from the two data sets (Figure 10) and their geographical (Figure 2) and temporal distribution are consistent with a robust sample. Student's t tests performed at each relevant pressure level indicate that the two data sets have significantly different means ($p < < 0.01$). However, bias values are well below the 10% accuracy specification for the MOPITT instrument [*Pan et al.*, 1995] and are also within the 10% retrieval error reported for ACE-FTS CO in the troposphere [*Clerbaux et al.*, 2008]. Thus, we conclude that the level of agreement between the two data sets in the upper troposphere is satisfactory. Reduced biases at the 100 hPa pressure level are consistent with MOPITT retrievals being at that level dominated by the a priori, which is obtained from the chemical transport model MOZART (Model for OZone and Related chemical Tracers) [*Emmons et al.*, 2010]. The difference between ACE-FTS measurements at low-pressure levels and the a priori (Figure 3) argues for a possible CO overestimation by the latter. Our results are, overall, consistent with those of *Clerbaux et al.* [2008], who in an analysis of MOPITT v3 and ACE-FTS v2.2 CO retrievals reported a 2.2% average discrepancy in the 5.5–15 km altitude range (roughly equivalent to 500–100 hPa), with retrievals from MOPITT being higher than those from ACE by that percentage.

Similarly, MOPITT retrievals are slightly higher than their HIPPO-QCLS counterparts at pressure levels between 200 and 400 hPa (from <4 to <14%, respectively, Figure 12); the bias at 500 hPa is close to −1%. Even though the number of paired measurements from the two data sets is rather limited (Figure 12), their geographical (Figures 4a–4d) and temporal distribution may be considered adequate. Student's t test results indicate that only at 300 hPa is the difference between the means of the two data sets statistically significant ($p = 0.003$). From our results, we conclude that MOPITT and HIPPO-QCLS CO values in the upper troposphere are in good agreement, except at 300 hPa, where MOPITT retrievals have a <14% positive bias. *Deeter et al.* [2013] report MOPITT v5 versus HIPPO-QCLS bias values for 200 and 400 hPa (10 and 4.7%) that are very similar to our results. Our calculated biases for pressure levels between 500 and 1000 hPa are below 4%, consistent with results from *Deeter et al.* [2013], showing exceptionally good agreement between the two data sets in the middle and low troposphere. The larger discrepancy between MOPITT retrievals and HIPPO-QCLS measurements at 200 and 300 hPa suggests a radiance bias for the MOPITT thermal pressure-modulated cell channel for which the weighting functions typically peak in the upper troposphere [*Drummond et al.*, 2010]. This radiance bias could, in turn, be related to instrument specifications or to issues in the temperature and/or water vapor profiles used in the retrieval process [*Deeter et al.*, 2013]. The thermal length modulation cell radiometer channels [*Drummond et al.*, 2010] utilized in MOPITT low and middle troposphere retrievals agree better with the model-simulated radiances, hence their good agreement with HIPPO at lower altitudes.
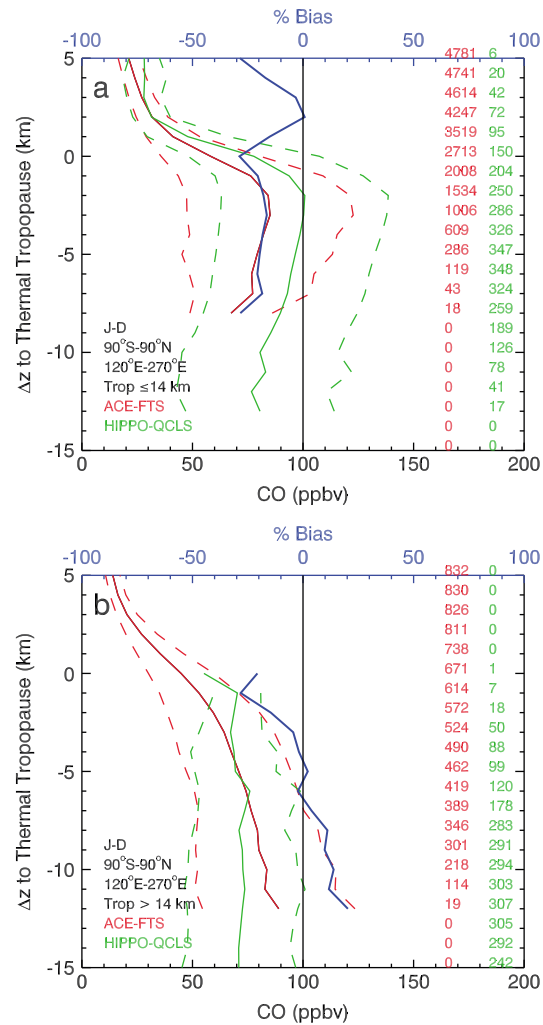
Figure 16. (a) Comparison between noncoincident ACE-FTS and HIPPO-QCLS extratropical CO profiles (i.e., profiles with tropopause at ≤14 km) relative to the thermal tropopause. Solid red and green lines show average CO profiles for ACE-FTS and HIPPO-QCLS, respectively. Dashed lines show ±1 standard deviation from the average. The number of measurements at each pressure level is shown color coded according to the instrument. The blue line indicates average percent bias between ACE-FTS and HIPPO-QCLS CO as a function of distance to the tropopause. Negative bias values indicate that ACE-FTS retrievals are lower than those from HIPPO-QCLS. JD = January to December. (b) Same for tropical profiles (i.e., profiles with tropopause at >14 km).

Direct profile comparisons between ACE-FTS and HIPPO-QCLS show that the ACE values are consistently lower than their smoothed counterparts (between −37 and −1% at ~170 and ~490 hPa, respectively, Figure 14). Student's t test results indicate though that the differences between the means of the two data sets at each relevant pressure level are not statistically significant ($p > 0.1$). Due to the very low number of coincident measurements (between 3 and 6 per pressure level analyzed) and subsequent inconclusive statistical results, we have applied two additional indirect techniques appropriate for the comparison of noncoincident observations: tracer-tracer (CO-O_3) correlation analysis and analysis of profiles relative to the thermal tropopause.

Qualitative tracer-tracer correlation analysis results indicate general agreement between the relative magnitudes of the tracers as measured by ACE-FTS and the HIPPO instruments (Figures 7 and 8a). *Hegglin et al.* [2008] report similar results when comparing ACE-FTS v2.2 CO retrievals and airborne SPURT CO measurements. We extended our analysis by producing ACE-FTS and HIPPO-QCLS CO frequency and cumulative frequency distributions (Figure 8b) for subsets of the data sets that maximize their spatial and temporal overlap, as explained in section 4.3. These indicate that albeit comparable, the distributions of CO
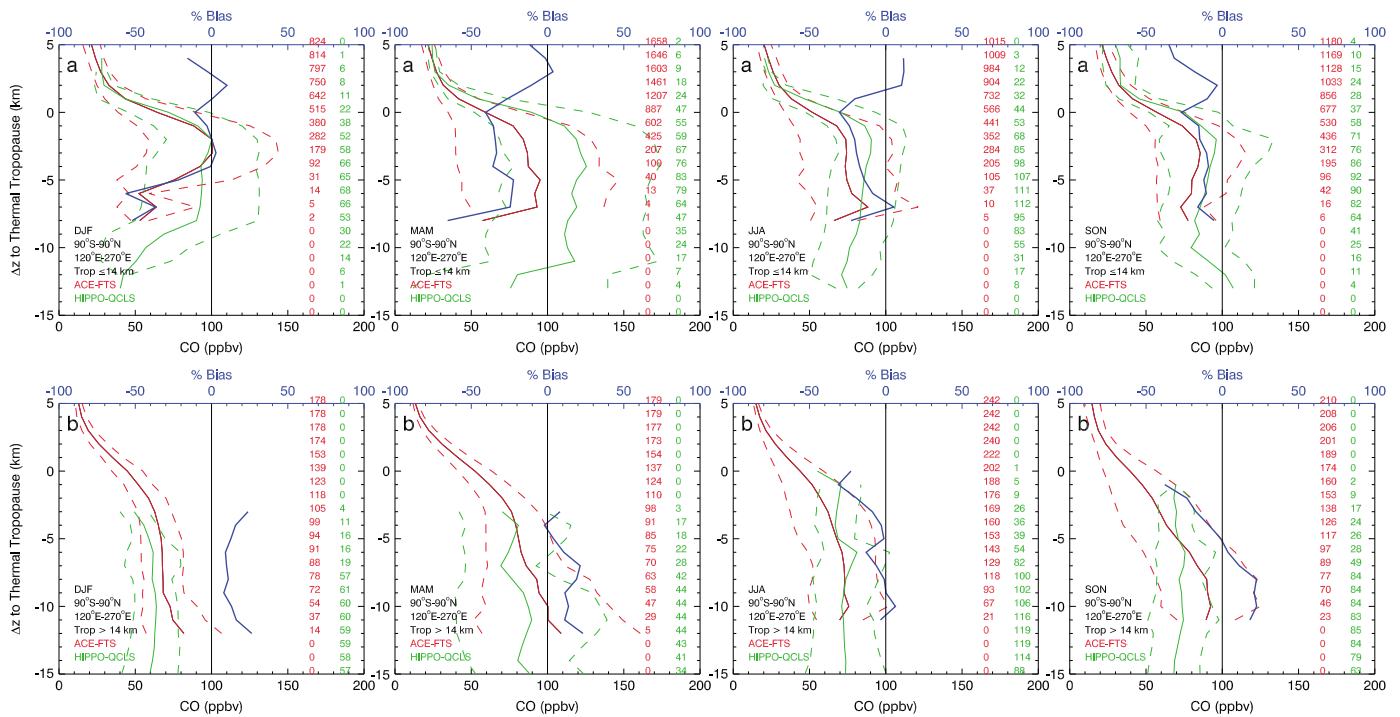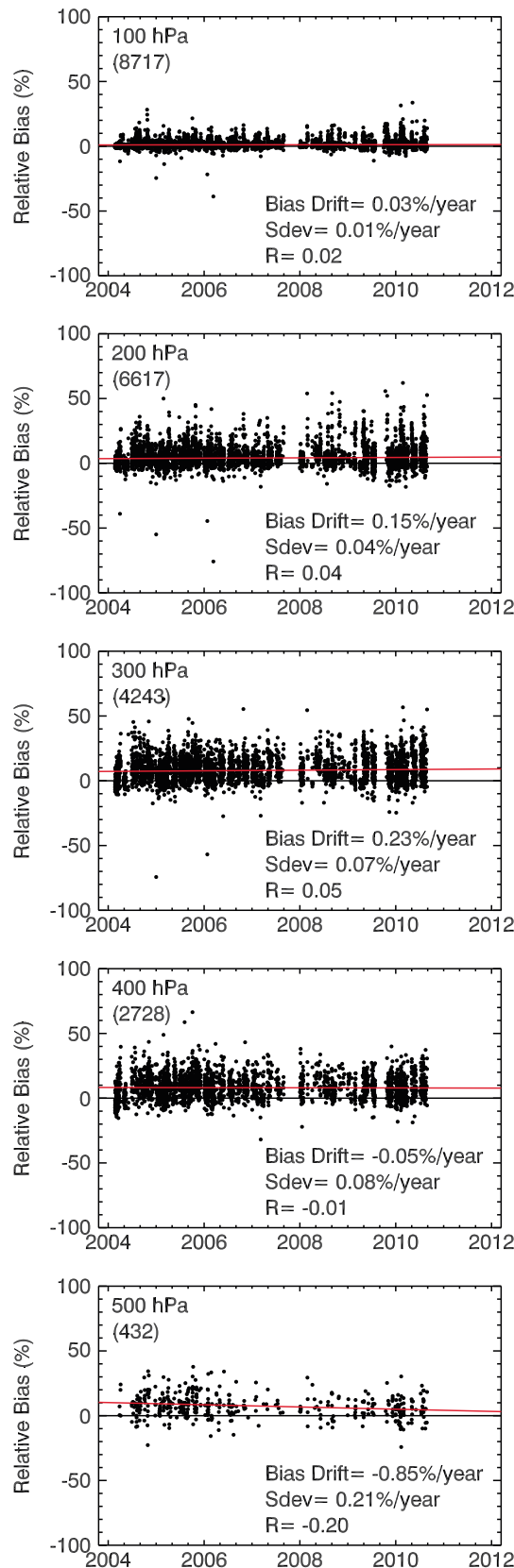
Figure 17. (a) Comparison between noncoincident ACE-FTS and HIPPO-QCLS extratropical CO profiles (i.e., profiles with tropopause at ≤14 km) relative to the thermal tropopause, segregated by season. (b) Same for tropical profiles (i.e., profiles with tropopause at >14 km). Negative bias values indicate that ACE-FTS retrievals are lower than those from HIPPO-QCLS. See caption of Figure16.

abundances retrieved from the two instruments differ. High CO values (~ >100 ppbv) are more frequent in the HIPPO-QCLS data set than in the ACE-FTS data set. This is consistent with HIPPO detecting high-CO plumes below the spatial resolution of ACE-FTS. Additionally, Student's t test results show that the difference between the means of the two data sets is statistically significant ($p \ll 0.01$).

Analysis of CO profiles in tropopause coordinates shows a generally negative bias of ACE-FTS with respect to HIPPO-QCLS between the tropopause and ~5 km below it (Figures 16 and 17). Student's t test results in most cases indicate that where the absolute value of bias is greater than ~10%, the differences between the two data sets are statistically significant ($p < 0.001$). We observe this in tropical and extratropical profiles, both segregating and not segregating the data by season. The magnitude of the bias is variable depending on the subset of data analyzed, their average being in the vicinity of −20%. In contrast, the bias at more than 5 km below the tropopause tends to be positive (i.e., ACE-FTS retrievals are higher than their HIPPO-QCLS counterparts) and smaller in magnitude, near +10%. It is unclear why profiles from the December−January−February season depart from this general behavior; this could result from stratospheric polar vortex effects or from some other winter-specific phenomena. In their analysis of profiles in tropopause coordinates, *Hegglin et al.* [2008] found that biases between upper tropospheric ACE-FTS v2.2 CO retrievals and airborne SPURT CO measurements were (on average) on the order of ±9%; nonaveraged bias values appear to be in the ±20% range [*Hegglin et al.*, 2008, Figure 11b]. Their analysis was restricted to latitudes between 40°N and 60°N; hence, most tropopauses were probably extratropical (i.e., lower than 14 km). According to *Hegglin et al.* [2008], the influence of the tropopause in shaping tracer distributions in the upper troposphere and lower stratosphere is limited to a certain depth that is a function of season (4 km below the tropopause in boreal winter and spring or 3 km in boreal summer and fall). If we exclude bias results below 4 km from the tropopause, our results indicate that upper tropospheric ACE-FTS CO retrievals are lower than HIPPO-QCLS measurements by 10 to 20%.

To sum up, the results suggest that although there is good overall agreement between the two data sets, upper tropospheric ACE-FTS retrievals appear, in general, lower than HIPPO-QCLS measurements. This conclusion is not supported by the relationships found in this study between MOPITT and ACE-FTS and between MOPITT and HIPPO-QCLS, according to which ACE-FTS retrievals and HIPPO-QCLS measurements should be very close. A possible cause for the apparent negative bias of ACE-FTS retrievals with respect

to HIPPO-QCLS could be the large differences in horizontal resolution between the two data sets (~300 km versus ~160 m). If HIPPO's finer horizontal resolution is not properly degraded, then the HIPPO data set is more likely to include high CO values which would get "diluted" (i.e., mixed with the background) at ACE's lower horizontal resolution. Similarly, differences in the vertical resolution of each instrument (~3–4 km versus 10 m) could contribute to the bias observed. Figure 14 shows that the statistics of presmoothing and postsmoothing biases are very similar, as expected from the triangular function smoothing technique. It is thus unclear whether this smoothing technique is sufficient for a proper comparison between the two data sets.

Deficiencies in the ACE-FTS CO retrievals below ~20 km of altitude cannot be ruled out either. Two bands are used in these retrievals: the 1-0 band near 2100 cm^{-1}, with signal-to-noise ratio (SNR) better than 300:1, and the 2-0 band near 4250 cm^{-1}, with SNR about 50:1. At low altitudes, the low-J lines in the 1-0 band saturate. Thus, for altitudes below ~15 to 13 km (at the equator and the poles, respectively), all the information comes from a set of 7 microwindows in the weak and noisy 2-0 band plus 1 microwindow containing a high-J line from the 1-0 band that extends down to 8 km. Because the latter has a much higher SNR than the former, it may exert an undue influence on the retrieval. Finally, some part of the observed differences between the ACE-FTS retrievals and the HIPPO measurements may result from actual differences in upper tropospheric CO concentrations caused by different sampling of discrete plumes, quasi-biennial oscillation effects, or polar vortex events, among others, since the averages analyzed do not encompass the same time periods.

The relative bias between upper tropospheric MOPITT and ACE-FTS CO retrievals appears to have remained stable between 2004 and 2010, the period for which relevant data from the two instruments are available at the time of writing (Figure 18). Very slight slopes in the bias trend for data at pressure levels between 100 and 400 hPa

Figure 18. Temporal trends in average percent bias between MOPITT and ACE-FTS CO retrievals as a function of MOPITT pressure level. Positive values indicate that MOPITT retrievals are higher than those from ACE-FTS. The number of individual bias measurements at each level is shown in parenthesis. Gaps correspond to ACE occultations lacking geolocation information for the individual measurements.

have been identified; albeit small, some of the slope values are statistically significant at the 99% confidence level. We estimate that these would result in exceedingly small changes in bias: 1% change each 4.3 years (at 300 hPa) to each 33 years (at 100 hPa). A slightly stronger, also statistically significant at the 99% confidence level, negative slope has been identified at 500 hPa; if not an artifact, this slope would result in a 0.85% decrease in bias per year. It is unclear if the smaller number of samples at 500 hPa may result in the slightly more pronounced slope. Our calculated bias trends (+0.15 and −0.05% bias/yr at 200 and 400 hPa, respectively) are noticeably smaller than those reported by *Deeter et al.* [2013] in a comparison of MOPITT v5 retrievals and NOAA in situ flask sampling measurements (+0.81 and +0.59% bias/yr at 200 and 400 hPa, respectively).

6. Summary and Conclusions

This study has shown that there is good agreement in upper tropospheric ($\leq$500 hPa) CO between MOPITT and ACE-FTS as well as between MOPITT and HIPPO-QCLS. Despite large differences in sampling resolution and observation types of these instruments, direct profile comparisons have been performed successfully. In general, biases between MOPITT and ACE-FTS as well as between MOPITT and HIPPO-QCLS are slight and positive (i.e., the MOPITT values are higher), albeit well within the expected 10% accuracy of MOPITT and ACE-FTS; only the bias between MOPITT and HIPPO-QCLS at 200 and 300 hPa ($<$14%) surpass that threshold. These comparisons will be performed next for MOPITT version 6 data, which are expected to have improved bias in the upper troposphere [*Deeter et al.*, 2014].

Direct profile comparisons between the ACE-FTS and HIPPO-QCLS data sets indicate that their relative biases are between −1 and −37% (ACE-FTS retrievals being lower); due to the small number of samples and poor geographic representation, we do not consider these results to be significant by themselves. Thus, two additional indirect techniques for comparison of noncoincident data sets have been applied: tracer-tracer (CO-O$_3$) correlation analysis and analysis of profiles in tropopause coordinates. Both suggest that upper tropospheric retrievals from the ACE-FTS data set are lower than the HIPPO-QCLS measurements. It is unclear if these apparent biases are due to differences between the horizontal resolution of the two data sets, insufficient smoothing of the HIPPO-QCLS data, deficiencies in the ACE-FTS CO retrievals below ~20 km of altitude, or to the instruments sampling actual differences in upper tropospheric CO. Investigating alternative smoothing techniques in the absence of ACE-FTS averaging kernels may allow for better, more reliable comparisons with higher-resolution data sets.

The stability of MOPITT-ACE relative biases through the period analyzed (2004–2010) suggests that it is reasonable to use both data sets for climate studies. A −0.85% per year change in MOPITT versus ACE-FTS bias at 500 hPa should be further investigated to discard causes other than instrumental drift, such as insufficient colocated measurements from both instruments at that pressure level. Thus, these data sets could be used to monitor and quantify global transport and exchange of CO in the upper troposphere–lower stratosphere and to assess temporal (seasonal and interannual) trends.

The results from this investigation demonstrate that the ACE-FTS CO data set will be an excellent addition in future MOPITT validation efforts for a better understanding of MOPITT retrievals in the upper troposphere. They also open the possibility for global measurement-based studies of CO dynamics between troposphere and stratosphere via joint analysis of overlapping, reliable data sets with well understood performance in the troposphere (e.g., MOPITT) and upper troposphere-stratosphere (e.g., ACE-FTS). These results also argue for the feasibility of joint assimilation of MOPITT and ACE-FTS CO data in dynamical models. This could result in better estimates of tropospheric-stratospheric CO dynamics than can be obtained from either the separate data sets or models alone. Data assimilation would also facilitate comparisons of these data sets since it would explicitly account for the differences in vertical sensitivity. The model used for data assimilation would eliminate uncertainties due to noncoincidence since it would act as a transfer function for the times and locations of one set of observations to another set.

References

Bernath, P. F., et al. (2005), Atmospheric Chemistry Experiment (ACE): Mission overview, *Geophys. Res. Lett.*, *32*, L15S01, doi:10.1029/2005GL022386.

Boone, C. D., R. Nassar, K. A. Walker, Y. Rochon, S. D. McLeod, C. P. Rinsland, and P. F. Bernath (2005), Retrievals for the atmospheric chemistry experiment Fourier transform spectrometer, *Appl. Opt.*, *44*(33), 7218–7231.

Boone, C. D., K. A. Walker, and P. F. Bernath (2013), Version 3 retrievals for the Atmospheric Chemistry Experiment Fourier Transform Spectrometer (ACE-FTS), in *The Atmospheric Chemistry Experiment ACE at 10: A Solar Occultation Anthology*, edited by P. F. Bernath, pp. 103–127, A. Deepak, Hampton, Va.

Clerbaux, C., et al. (2008), CO measurements from the ACE-FTS satellite instrument: Data analysis and validation using ground-based, airborne and spaceborne observations, *Atmos. Chem. Phys.*, 8, 2569–2594, doi:10.5194/acp-8-2569-2008.

Deeter, M. N., et al. (2003), Operational carbon monoxide retrieval algorithm and selected results for the MOPITT instrument, *J. Geophys. Res.*, 108(D14), 4399, doi:10.1029/2002JD003186.

Deeter, M. N., D. P. Edwards, and J. C. Gille (2007), Retrievals of carbon monoxide profiles from MOPITT observations using lognormal a priori statistics, *J. Geophys. Res.*, 112, D11311, doi:10.1029/2006JD007999.

Deeter, M. N., et al. (2010), The MOPITT version 4 CO product: Algorithm enhancements, validation, and long-term stability, *J. Geophys. Res.*, 115, D07306, doi:10.1029/2009JD013005.

Deeter, M. N., S. Martínez-Alonso, D. P. Edwards, L. K. Emmons, J. C. Gille, H. M. Worden, J. V. Pittman, B. C. Daube, and S. C. Wofsy (2013), Validation of MOPITT Version 5 thermal-infrared, near-infrared, and multispectral carbon monoxide profile retrievals for 2000–2011, *J. Geophys. Res. Atmos.*, 118, 6710–6725, doi:10.1002/jgrd.50272.

Deeter, M. N., S. Martínez-Alonso, D. P. Edwards, L. K. Emmons, J. C. Gille, H. M. Worden, C. Sweeney, J. V. Pittman, B. C. Daube, and S. C. Wofsy (2014), The MOPITT Version 6 product: Algorithm enhancements and validation, *Atmos. Meas. Tech.*, 7, 3623–3632, doi:10.5194/amt-7-3623-2014.

Drummond, J. R., and G. S. Mand (1996), The measurements of pollution in the troposphere (MOPITT) instrument: Overall performance and calibration requirements, *J. Atmos. Oceanic Technol.*, 13(2), 314–320, doi:10.1175/1520-0426.

Drummond, J. R., J. Zou, F. Nichitiu, J. Kar, R. Deschambaut, and J. Hackett (2010), A review of 9-year performance and operation of the MOPITT instrument, *Adv. Space Res.*, 45, 760–774, doi:10.1016/j.asr.2009.11.019.

Dupuy, E., et al. (2009), Validation of ozone measurements from the Atmospheric Chemistry Experiment (ACE), *Atmos. Chem. Phys.*, 9, 287–343. [Available at www.atmos-chem-phys.net/9/287/2009/.]

Emmons, L. K., et al. (2004), Validation of Measurements of Pollution in the Troposphere (MOPITT) CO retrievals with aircraft in situ profiles, *J. Geophys. Res.*, 109, D03309, doi:10.1029/2003JD004101.

Emmons, L. K., G. G. Pfister, D. P. Edwards, J. C. Gille, G. Sachse, D. Blake, S. Wofsy, C. Gerbig, D. Matross, and P. Nédélec (2007), Measurements of Pollution In The Troposphere (MOPITT) validation exercises during summer 2004 field campaigns over North America, *J. Geophys. Res.*, 112, D12S02, doi:10.1029/2006JD007833.

Emmons, L. K., D. P. Edwards, M. N. Deeter, J. C. Gille, T. Campos, P. Nédélec, P. Novelli, and G. Sachse (2009), Measurements of Pollution in the Troposphere (MOPITT) validation through 2006, *Atmos. Chem. Phys.*, 9(5), 1795–1803, doi:10.5194/acp-9-1795-2009.

Emmons, L. K., et al. (2010), Description and evaluation of the Model for Ozone and Related chemical Tracers, version 4 (MOZART-4), *Geosci. Model Dev.*, 3, 43–67. [Available at www.geosci-model-dev.net/3/43/2010/.]

Fischer, H., F. G. Wienhold, P. Hoor, O. Bujok, C. Schiller, P. Siegmund, M. Ambaum, H. A. Scheeren, and J. Lelieveld (2000), Tracer correlations in the northern high latitude lowermost stratosphere: Influence of cross-tropopause mass exchange, *Geophys. Res. Lett.*, 27, 97–100, doi:10.1029/2000JD900288.

Heald, C. L., et al. (2003), Asian outflow and trans-Pacific transport of carbon monoxide and ozone pollution: An integrated satellite, aircraft, and model perspective, *J. Geophys. Res.*, 108(D24), 4804, doi:10.1029/2003JD003507.

Hegglin, M. I., C. D. Boone, G. L. Manney, T. G. Shepherd, K. A. Walker, P. F. Bernath, W. H. Daffer, P. Hoor, and C. Schiller (2008), Validation of ACE-FTS satellite data in the upper troposphere/lower stratosphere (UTLS) using non-coincident measurements, *Atmos. Chem. Phys.*, 8, 1483–1499, doi:10.5194/acp-8-1483-2008.

Hegglin, M. I., C. D. Boone, G. L. Manney, and K. A. Walker (2009), A global view of the extratropical tropopause transition layer from Atmospheric Chemistry Experiment Fourier Transform Spectrometer O_3, H_2O, and CO, *J. Geophys. Res.*, 114, D00B11, ISSN 0148-0227, doi:10.1029/2008JD009984.

Jacob, D. J. (1999), *Introduction to Atmospheric Chemistry*, 264 pp., Princeton Univ. Press, Princeton, N. J.

Jiang, Z., D. B. A. Jones, H. M. Worden, M. N. Deeter, D. K. Henze, J. Worden, K. W. Bowman, C. A. M. Brenninkmeijer, and T. J. Schuck (2013), Impact of model errors in convective transport on CO source estimates inferred from MOPITT CO retrievals, *J. Geophys. Res. Atmos.*, 118, 2073–2083, doi:10.1002/jgrd.50216.

Jones, A., et al. (2012), Technical Note: A trace gas climatology derived from the Atmospheric Chemistry Experiment Fourier Transform Spectrometer (ACE-FTS) data set, *Atmos. Chem. Phys.*, 12, 5207–5220, doi:10.5194/acp-12-5207-2012. [Available at www.atmos-chem-phys.net/12/5207/2012/.]

Manney, G. L., et al. (2007), Solar occultation satellite data and derived meteorological products: Sampling issues and comparisons with Aura Microwave Limb Sounder, *J. Geophys. Res.*, 112, D24S50, doi:10.1029/2007JD008709.

Manney, G. L., et al. (2011), Jet characterization in the upper troposphere/lower stratosphere (UTLS): Applications to climatology and transport studies, *Atmos. Chem. Phys.*, 11, 6115–6137, doi:10.5194/acp-11-6115-2011.

McManus, J. B., M. S. Zahniser, D. D. Nelson, J. H. Shorter, S. Herndon, E. Wood, and R. Wehr (2010), Application of quantum cascade lasers to high-precision atmospheric trace gas measurements, *Opt. Eng.*, 49(11), 111124.1–111124.11, doi:10.1117/1.3498782.

Myhre, G., et al. (2013), Anthropogenic and natural radiative forcing, in *Climate Change 2013: The Physical Science Basis. Contribution of Working Group I to the Fifth Assessment Report of the Intergovernmental Panel on Climate Change*, edited by T. F. Stocker et al., Cambridge Univ. Press, Cambridge, U. K., and New York.

Pan, L., D. P. Edwards, J. C. Gille, M. W. Smith, and J. R. Drummond (1995), Satellite remote sensing of tropospheric CO and CH_4: Forward model studies of the MOPITT instrument, *Appl. Opt.*, 34, 6976–6988.

Pan, L. L., W. J. Randel, B. L. Gary, M. J. Mahoney, and E. J. Hintsa (2004), Definitions and sharpness of the extratropical tropopause: A trace gas perspective, *J. Geophys. Res.*, 109, D23103, doi:10.1029/2004JD004982.

Pan, L. L., J. C. Wei, D. E. Kinnison, R. R. García, D. J. Wuebbles, and G. P. Brasseur (2007), A set of diagnostics for evaluating chemistry-climate models in the extratropical tropopause region, *J. Geophys. Res.*, 111, D09316, doi:10.1029/2006JD007792.

Proffitt, M. H., and R. J. McLaughlin (1983), Fast-response dual-beam UV absorption ozone photometer suitable for use on stratospheric balloons, *Rev. Sci. Instrum.*, 54, 1719–1728.

Randel, W. J., M. Park, F. Wu, and N. Livesey (2007), A large annual cycle in ozone above the tropical tropopause linked to the Brewer–Dobson circulation, *J. Atmos. Sci.*, 64, 4479–4488, doi:10.1175/2007JAS2409.1.

Rodgers, C. D., and B. J. Connor (2003), Intercomparison of remote sounding instruments, *J. Geophys. Res.*, 108(D3), 4116, doi:10.1029/2002JD002299.

Santoni, G. W., et al. (2013), Evaluation of the Airborne Quantum Cascade Laser Spectrometer (QCLS) measurements of the carbon and greenhouse gas suite—CO_2, CH_4, N_2O, and CO—during the CalNex and HIPPO campaigns, *Atmos. Meas. Tech. Discuss.*, *6*, 9689–9734, doi:10.5194/amtd-6-9689-2013.

Schoeberl, M. R., B. N. Duncan, A. R. Douglass, J. Waters, N. Livesey, W. Read, and M. Filipiak (2006), The carbon monoxide tape recorder, *Geophys. Res. Lett.*, *33*, L12811, doi:10.1029/2006GL026178.

Tereszchuk, K. A., G. G. Abad, C. Clerbaux, D. Hurtmans, P.-F. Coheur, and P. F. Bernath (2011), ACE-FTS measurements of trace species in the characterization of biomass burning plumes, *Atmos. Chem. Phys.*, *11*, 12,169–12,179, doi:10.5194/acp-11-12169-2011.

Tilmes, S., et al. (2010), An aircraft-based upper troposphere lower stratosphere O_3, CO, and H_2O climatology for the Northern Hemisphere, *J. Geophys. Res.*, *115*, D14303, doi:10.1029/2009JD012731.

Wofsy, S. C., et al. (2011), HIAPER Pole-to-Pole Observations (HIPPO): Fine-grained, global-scale measurements of climatically important atmospheric gases and aerosols, *Phil. Trans. R. Soc.*, *369*(1943), 2073–2086, doi:10.1098/rsta.2010.0313.

Worden, H. M., M. N. Deeter, D. P. Edwards, J. C. Gille, J. R. Drummond, and P. Nédélec (2010), Observations of near-surface carbon monoxide from space using MOPITT multispectral retrievals, *J. Geophys. Res.*, *115*, D18314, doi:10.1029/2010JD014242.

Worden, H. M., M. N. Deeter, D. P. Edwards, J. Gille, J. Drummond, L. K. Emmons, G. Francis, and S. Martínez-Alonso (2014), 13 years of MOPITT operations: Lessons from MOPITT retrieval algorithm development, *Ann. Geophys.*, *56*(0), doi:10.4401/ag-6330.

World Meteorological Organization (1957), Meteorology—A three-dimensional science, 230, *WMO Bull.*, *6*, 134–138.